Int. J. Solids Structures, 1975, Vol 11, pp. 1035–1049. Pergamon Press. Printed in Gt. Britain.

SNAP-THROUGH BUCKLING OF ECCENTRICALLY STIFFENED SHALLOW SPHERICAL CAPS

GEORGE J. SIMITSES†
Georgia Institute of Technology, Atlanta, GA 30332, U.S.A.

and

CHARLES M. BLACKMON
United States Weapons Laboratory, Dahlgren, Virginia, U.S.A.

(*Received* 4 *November* 1974; *Revised* 10 *February* 1975)

Abstract—The problem of snap-through buckling of a clamped, eccentrically stiffened shallow spherical cap is considered under quasi-statically applied uniform pressure and a special case of dynamically applied uniform pressure. This dynamic case is the constant load infinite duration case (step time-function) and it represents an extreme case of blast loading-large decay time, small decay rate.

The analysis is based on the nonlinear shallow shell equations under the assumption of axisymmetric deformations and linear stress-strain laws. The eccentric stiffeners are disposed orthogonally along directions of principal curvature in such a way that the smeared mass, and extensional and flexural stiffnesses are constant. The stiffeners are also taken to be one-sided with constant eccentricity, and the stiffener-shell connection is assumed to be monolithic.

The method developed in an earlier paper is employed. In this method, critical pressures are associated with characteristics of the total potential surface in the configuration space of the generalized coordinates.

In addition, buckling of the complete thin eccentrically stiffened spherical shell under uniform quasi-statically applied pressure is considered, and these results are used to check the numerical answers. The complete spherical shell is stiffened in the same manner as the shallow cap.

The results are presented in graphical form as load parameter vs initial rise parameter. Geometric configurations corresponding to isotropic, lightly stiffened, moderately stiffened and heavily stiffened geometries are considered. By lightly stiffened geometry one means that most of the extensional stiffness is provided by the thin shell. A computer program was written to solve for critical pressures. The Georgia Tech Univac 1108 high speed digital computer was used for this purpose.

NOTATION

a	Radius to the reference surface of a thin spherical shell, in
A_r, A_θ	Cross-sectional area of the stiffeners, inch^2
D	Flexural stiffness of the sheet, inch-lbs
D^s	Smeared flexular stiffness of the stiffeners, inch-lbs
E^p, E^s	Extensional stiffnesses of the sheet and stiffeners respectively, lbs/in
e	Stiffener eccentricity, in
E, E_r, E_θ	Young's modulus for sheet and stiffeners, psi
h	Sheet thickness, in
H	Rise of the sheet midsurface, in
I_r, I_θ	Second moment of stiffener area about own centroidal axes, in^4
l_r, l_θ	Stiffener spacings, in
$M_r, M_\theta, M_{r\theta}$	Stiffened shell moment resultants, lbs
$N_r, N_\theta, N_{r\theta}$	Stiffened shell stress resultants, lbs/in
q	Applied pressure, psi
Q	Nondimensionalized applied pressure
r, θ	Polar coordinates
T	Kinetic energy, lb-inches
T_d	Kinetic energy volume density, psi
U_T	Total potential, lb-inches
U_{T_d}	Total potential volume density, psi
u, v, w	Displacement components of the reference surface, in
z	Distance to the undeformed reference surface (from the boundary plane, $r\theta$-plane) in
$\epsilon_{rr}, \epsilon_{\theta\theta}, \gamma_{r\theta}$	Reference surface strains
η	Nondimensionalized normal displacement component
$k_{rr}, k_{\theta\theta}, k_{r\theta}$	Changes in curvature and torsion at the reference surface. (per inch)
λ	Initial rise parameter $\left\{ = 2[3(1-\nu^2)]^{1/4}\left(\frac{H}{h_{eq}}\right)^{1/2} \right\}$
λ_0	Ratio of extensional stiffnesses (stiffener to sheet)
ν	Poisson's ratio

†Professor, School of Engineering Science and Mechanics.

ρ Ratio of the pressure at which the cap loses stability to the classical critical pressure for a complete sphere of thickness h
ρ_0 Ratio of flexural stiffnesses (stiffener to sheet)
ξ Dimensionless radial distance
ψ Stress function in polar co-ordinates (lb-in)
∇^2 Laplacian operator in polar co-ordinates

1. INTRODUCTION

The need for structural efficiency in aircraft and missile structures is a well recognized fact. Thus structural instability, which can lead to failure, is a serious problem. Since thin-walled shallow spherical caps have many uses in modern aerospace structures, the question of how to make the most effective use of the material employed in their construction is important. Within the past several years studies have shown that eccentrically stiffened shells could be one answer to this problem. Typically, Harari, Singer and Baruch[1] showed that by using eccentric stiffeners the buckling load to weight ratio of axially compressed circular cylinders could be increased by as much as 50%.

Structural elements are often subjected to both quasi-static and dynamic lateral loads which act toward the center of curvature. The typical response to such loading in shallow caps is snap-through buckling or oil canning and is characterized by a visible and sudden jump from one equilibrium configuration to another for which the displacements are larger than in the first. For the loading to be considered quasi-static, the time rate of load application must be of such magnitude that significant dynamic effects are not induced. However, dynamic load application causes significant inertia effects which can substantially modify the critical conditions compared to the quasi-static case. Thus, a knowledge of the behavior in both circumstances is most desirable.

A large amount of experimental and analytical work has been done on the stability of monocoque cylindrical and spherical shells and on eccentrically stiffened cylindrical shells. Recently, Cole[2] performed a comprehensive parametric study of the effect of eccentric stiffeners on the buckling of complete spheres and indicated that considerable weight savings can be realized. His work also contains an excellent bibliography concerning eccentric stiffening effects on thin shells from the time the effects were first recognized by Van der Neut[3] to the present. There are, however, only a few studies, both analytical and experimental, of the buckling characteristics of spherical caps with non-uniform wall construction, and in these studies consideration was given only to quasi-static loading.

The study of the elastic stability of thin shallow isotropic spherical shells subjected to uniform pressure dates back to the investigations of von Kármán and Tsien[4]. Suhara[5] gives an historical summary of pertinent research prior to 1960. In more recent times, the critical impulse has been calculated by Humphreys and Bodner[6] using the Rayleigh–Ritz method. The same problem was also studied by Budiansky and Roth[7] using the Galerkin method. At the same time Budiansky and Roth solved the problem of dynamic snap-through under instantaneously applied uniform pressure with infinite duration and reported results for a particular value of height-thickness ratio. Archer and Lange[8] treated this problem numerically by replacing the governing differential equations by finite difference equations.

Simitses[9] used a Ritz type procedure to find both the minimum possible dynamic load and impulse for snap-through for a wide range of the height to thickness parameter. Experimentally, Lock, Okubo and Whittier[10] measured the dynamic snap-through load for two values of the height-thickness ratio in which complete axisymmetric behavior was observed during snap-through. In recent works both Stephens and Fulton[11] and Stricklin and Martinez[12] determined critical snap-through loads which are in good agreement for a wide range of height-thickness ratios. These authors used finite difference and finite element displacement methods respectively. Huang[13], in a recent paper, integrated the non-linear differential equations by a finite difference method and an iterative procedure. He found critical loads for dynamic snap-through that are in good agreement with the results of the two last mentioned investigations[11–12].

Additional references on the subject may be found in a review article by Simitses[14] in 1974. Finally, for the sake of completeness, the reader is referred to a number of publications[15–21] which deal with similar aspects of the problem, both analytically and experimentally, through 1974.

The buckling of a clamped eccentrically stiffened spherical cap under quasi-static loading has been investigated by Bushnell [22–23] in recent papers using a finite difference technique. He, however, did not present an extensive parametric study of the stiffener eccentricity effect. Several other authors have made studies of the stability of eccentrically stiffened spherical domes under quasi-static loading. Ebner [24] used an approximate method to calculate the general instability loads of meridionally stiffened shallow domes under uniform external pressure. In this work no account was taken of stiffener eccentricity. Crawford and Schwartz [25] calculated bifurcation loads from a membrane state for grid-stiffened spherical domes. They idealized the structure by considering it orthotropic and by neglecting the eccentricity of the stiffeners. In a later analysis, Crawford [26] derived constitutive relations in which the effect of eccentricity was included.

The problem, to be considered in this paper, is the definition and analysis of axisymmetric snap-through buckling for an eccentrically stiffened clamped shallow spherical cap under quasi-statically applied uniform pressure and one special case of dynamically applied uniform pressure; instantaneously applied step (Heaviside function) loading with infinite duration.

2. TECHNICAL APPROACH

The method to be employed is similar to that used by Simitses [9] for the clamped isotropic shallow shell. A Ritz–Galerkin procedure is used for the quasi-static case, and a modified Ritz–Galerkin procedure is employed for the dynamic case. The two methods are approximate and from the quasi-static buckling problem of shallow caps, as observed by Budiansky [27], it was found that the buckling load derived from an energy method deviates from the exact solution somewhat. He noted that this deviation increases with increases in the height-thickness ratios of the shell. It is necessary, therefore, to examine the results obtained by this method as to their range of applicability.

All load cases considered do not explicitly depend on time and exhibit such a load behavior that the total mechanical system is conservative. Therefore Hamilton's integral, I, may be written as

$$I = \int_{t_1}^{t_2} \left[\iint_{V_{ol}} (T_d - U_{T_d}) \mathrm{d}V \right] \mathrm{d}t \tag{1}$$

where T_d is the kinetic energy volume density and U_{T_d} is the total potential energy volume density. It should be noted that T_d and U_{T_d} may be expressed solely in terms of the displacement components u, v and w in the plane and normal to the plane of the circular boundary.

In the derivation of the kinetic and total potential energy volume densities the following assumptions are made: (i) The deformation is axisymmetric. (ii) The effect of transverse shear forces on the deformation is negligible. (iii) Rotatory and in-plane kinetic energies are considered small compared to the normal kinetic energy. The last assumption was justified by Reissner [28, 29] for the isotropic shell. Although the inclusion of stiffeners does add to the rotatory and in-plane energy, it is felt that these terms can still be considered small in relation to the normal kinetic energy. By neglecting these terms the critical loads found in this analysis will be somewhat conservative.

Applying Hamilton's principle, the extremization of (1) with respect to u and v yields the in-plane equation of motion (in-plane equilibrium). These equations are not explicitly dependent on time because of assumption (iii). The third, equilibrium equation is obtained by setting the generalized velocities equal to zero and performing the extrimization with respect to w.

A finite series of space-dependent functions with time-dependent (in general) coefficients is assumed to represent the normal displacement w with each term of the series satisfying the prescribed boundary conditions. By assuming the deflection shape a priori, the internal elastic strain energy may be associated with the shape amplitudes in the following manner: A stress function is used which identically satisfies in-plane equilibrium. Through the compatibility equation and associated boundary conditions, the stress function is related to the normal displacement w. Using this relation in the expression for the total potential yields the total potential surface in terms of the normal displacement w only. The time-dependent coefficients are analogous to generalized coordinates, and the total potential is thus a function of the loading, overall structural geometry and the generalized coordinates, a_i.

Setting the generalized velocities equal to zero and applying the principle of the stationary value of the total potential gives the static equilibrium points of a conservative system. This implies

$$\frac{\partial U_T}{\partial a_i} = 0 \qquad i = 1, 2, \ldots \tag{2}$$

at every static equilibrium point. Critical pressures for this case are obtained by considering the stability, in the small, of these equilibrium points through second variations. A snapping phenomenon is possible if the total potential surface in the space of the generalized coordinates has at least three static equilibrium points of which two are stable (one near and one far). The pressure is critical, when the near equilibrium point becomes unstable[9].

In considering the case of constant load with infinite duration, it is noted that for conservative and stationary systems the Hamiltonian is constant.

$$T + U_T = \text{constant} \tag{3}$$

The total potential can be defined such that, if the initial kinetic energy is zero, the constant will be zero.

$$T + U_T = 0 \tag{4}$$

Since the kinetic energy is a positive definite quantity, the presence of buckled or unbuckled motion can be determined by examining the total potential surface.

The following definitions are needed for establishing the method used in this load case.

Possible locus: A possible locus on the total potential surface is one which corresponds at every point of the locus to a non-negative kinetic energy.

Unbuckled motion: Unbuckled motion of the system is defined as any possible locus on the total potential surface which completely encloses only the near equilibrium point.

Buckled motion: If the possible locus passes through or encloses other equilibrium points, or, if the near equilibrium point becomes unstable, the motion is defined as buckled, and the system has "snapped through".

Minimum possible critical load: The least upper bound of loads for which all possible loci correspond only to unbuckled motion. At this load there exists at least one possible locus on the total potential surface which the structure can follow to "snap-through". Thus the minimum possible critical load for this case is obtained by solving simultaneously eqns (2) and

$$U_T = 0 \tag{5}$$

at the unstable static equilibrium point.

As pointed out by Humphreys[30], the critical dynamic load obtained by the energy method may not be correct. However, it will now be shown that the result obtained by this method will always be a lower bound for the critical load. As the load increases in magnitude, the level of the total potential corresponding to the unstable static equilibrium points decreases. Let q_D represent the magnitude of external load for which the value of the total potential at one static equilibrium point is zero and a possible locus to that unstable point exists. Now, if $q < q_D$, there are two possibilities, either (i) all unstable equilibrium points have positive total potential energy, which case there is no possible locus to those points, or (ii) some unstable static equilibrium points might correspond to a nonpositive potential but there is no possible locus. In no circumstance is there a way for the system to reach an unstable static equilibrium point if $q < q_D$. Therefore, q_D represents a lower bound on external loads for snap-through.

One more point should be noted. The energy method provides true lower bounds only for the mechanical system whose energy is actually formulated. Thus, if a continuous system is approximated by an "n" degree of freedom discrete system, and the energy is then formulated for that discrete system, the resulting lower bounds are true only for the discrete system. The extent of applicability of the discrete system bounds to the continuous system depends on the accuracy of the approximation.

In this paper, the applicability of the results has been judged by comparisons with data derived from the "exact" solutions for the isotropic shell.

3. GOVERNING EQUATIONS FOR THE STIFFENED CAP

The thin shallow spherical cap is stiffened eccentrically in the circumferential and meridional directions as shown in Fig. 1 such that (i) the stiffeners are both on the same side, (ii) the stiffener eccentricity is the same for all stiffeners and constant, and (iii) the smeared extensional and flexural stiffnesses are the same along both the circumferential and meridional directions and constant.

The basic geometry and notation for a clamped shallow spherical cap is shown in Figs. 1 and 2. The nonlinear strain-displacement and curvature-displacement relations known as the shallow shell or Marguerre equations are taken from Sanders[31]. These equations are based on the assumptions of (i) small strains, (ii) moderately small rotations with rotations about the normal being neglected, and (iii) the Donnell–Mushtari–Vlasov approximation being made. In addition, it is assumed that the shell deforms in an axisymmetric mode. Under these assumptions the

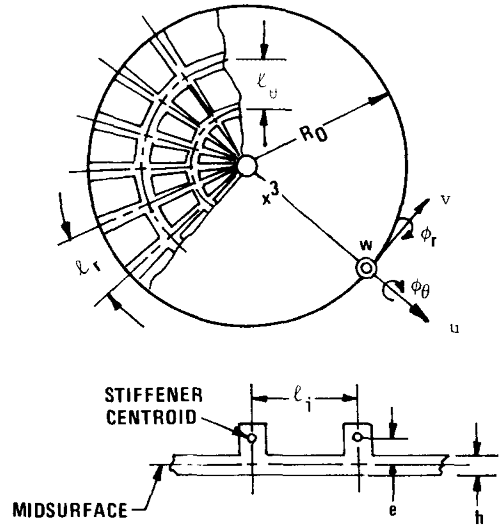

Fig. 1. Geometry.

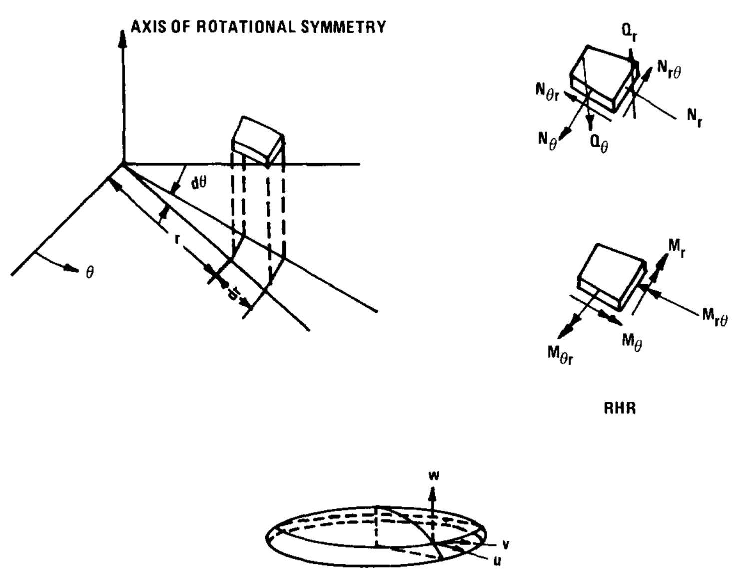

Fig. 2. Sign convention.

following basic kinematic relations can be written using the midsurface of the sheet as the reference.

$$\epsilon_{rr} = u_{,r} + z_{,r}w_{,r} + \frac{1}{2}(w_{,r})^2 \qquad \epsilon_{\theta\theta} = \frac{u}{r} \qquad \gamma_{r\theta} = 0 \tag{6}$$

$$k_{rr} = -w_{,rr}; \qquad k_{\theta\theta} = -\frac{1}{r}w_{,r}; \qquad k_{r\theta} = 0 \tag{7}$$

In the derivation of the constitutive relations for the combined sheet-stiffener system, as shown in Fig. 1, the Kirchhoff–Love hypotheses as modified by Baruch and Singer[32] are used. They assume that the stiffeners are close enough to be smeared and that they follow lines of principal curvature. The eccentricity effect, or height of the stiffener center of gravity above the midsurface, is retained by assuming that the strain varies linearly through the actual thickness of the stiffeners and not through a smeared-out or "effective" thickness. The "integrated" constitutive relations are

$$\begin{aligned} N_r &= (E^p + E_r^s)\epsilon_{rr} + \nu E^p\epsilon_{\theta\theta} + e_rE_r^sk_{rr} \\ N_\theta &= \nu E^p\epsilon_{rr} + (E^p + E_\theta^s)\epsilon_{\theta\theta} + e_\theta E_\theta^sk_{\theta\theta} \\ N_{r\theta} &= \frac{Eh}{2(1+\nu)}\gamma_{r\theta} \end{aligned} \tag{8}$$

$$\begin{aligned} M_r &= (D + D_r^s)k_{rr} + \nu Dk_{\theta\theta} + e_r^2E_r^sk_{rr} + e_rE_r^s\epsilon_{rr} \\ M_\theta &= \nu Dk_{rr} + (D + D_\theta^s)k_{\theta\theta} + e_\theta^2E_\theta^sk_{\theta\theta} + e_\theta E_\theta^s\epsilon_{\theta\theta} \\ M_{r\theta} &= D(1-\nu)k_{r\theta} \end{aligned} \tag{9}$$

where

$$E^p = \frac{Eh}{1-\nu^2}; \qquad E_r^s = \frac{E_rA_r}{l_r}; \qquad E_\theta^s = \frac{E_\theta A_\theta}{l_\theta}$$

$$D_\theta^s = \frac{E_\theta I_{\theta_{cg}}}{l_\theta}; \qquad D_r^s = \frac{E_rI_{r_{cg}}}{l_r}; \qquad D = \frac{Eh^3}{12(1-\nu^2)}. \tag{10}$$

A_i and $I_{i_{cg}}$ are the cross-sectional area and the second moment of the area about centroidal axes of the stiffeners respectively.

Next, if A_r and $I_{r_{cg}}$ are taken to vary linearly in the plane of (u and v), as l_r does, then E_r^s and D_r^s are constant. Furthermore, letting $E_r^s = E_\theta^s = E^s D_r^s = D_\theta^s = D^s$ and $e_r = e_\theta = e$ eqns (8) and (9) become

$$\begin{aligned} N_r &= (E^p + E^s)\epsilon_{rr} + \nu E^p\epsilon_{\theta\theta} + eE^sk_{rr} \\ N_\theta &= \nu E^p\epsilon_{rr} + (E^p + E^s)\epsilon_{\theta\theta} + eE^sk_{\theta\theta} \\ N_{r\theta} &= 0 \end{aligned} \tag{11}$$

$$\begin{aligned} M_r &= (D + D^s)k_{rr} + \nu Dk_{\theta\theta} + e^2E^sk_{rr} + eE^s\epsilon_{rr} \\ M_\theta &= \nu Dk_{rr} + (D + D^s)k_{\theta\theta} + e^2E^sk_{\theta\theta} + eE^s\epsilon_{\theta\theta} \\ M_{r\theta} &= 0. \end{aligned} \tag{12}$$

On the basis of the assumptions made, the following expressions may be written for the energies

$$T = \pi\sigma h\int_0^R w_{,t}^2 r\,dr \tag{13}$$

$$U_T = 2\pi\int_0^R (\bar{U} - qw)r\,dr \tag{14}$$

where $\bar{U}$ is the strain energy density function

$$\bar{U} = \frac{1}{2}(N_r\epsilon_{rr} + N_\theta\epsilon_{\theta\theta} + M_r k_{rr} + M_\theta k_{\theta\theta}) \tag{15}$$

and q is the applied uniform pressure positive in the positive w direction. Next, a stress function, ψ, is introduced which satisfies identically the in-plane equilibrium equation

$$N_\theta - (rN_r)_{,r} = 0 \tag{16}$$

and

$$N_r = \frac{1}{r}\psi_{,r} \qquad N_\theta = \psi_{,rr}. \tag{17}$$

The compatibility equation for the cap under the assumption of rotationally symmetric deformations and initial midsurface shape characterized by $z = z(r)$ is as follows:

$$(1+\lambda_0)\nabla^4\psi = e\lambda_0\nu E^p\nabla_w^4 - E^p[(1+\lambda_0)^2 - \nu^2]\left[\frac{1}{r}w_{,r}(z_{,rr} + w_{,rr}) + \frac{1}{r}w_{,r}z_{,r}\right] \tag{18}$$

where

$$\lambda_0 = \frac{E^s}{E^p}; \qquad \rho_0 = \frac{D^s}{D}; \qquad \nabla^4 = \frac{d^4}{dr^4} + \frac{2}{r}\frac{d^3}{dr^3} - \frac{1}{r^2}\frac{d^2}{dr^2} + \frac{1}{r^3}\frac{d}{dr}$$

The boundary conditions at $r = R$ are:

$$w = 0 \qquad w_{,r} = 0 \qquad u = 0 \qquad v = 0 \tag{19}$$

The last two of these boundary conditions can be expressed solely in terms of w and the stress function ψ following the steps outlined by Huang[33].

At $r = R$

$$\psi_{,rr} - \frac{\nu}{1+\lambda_0}\frac{1}{R}\psi_{,r} = \frac{eE^s\nu}{1+\lambda_0}w_{,rr} \tag{20a}$$

$$\psi_{,rrr} - \frac{1}{R^2}\left(\frac{1+\lambda_0-\nu}{1+\lambda_0}\right)\psi_{,r} = \frac{eE^s\nu}{1+\lambda_0}w_{,rrr} \tag{20b}$$

In addition, the auxiliary condition that all stresses and displacements at the center ($r = 0$) of the shell must remain finite is also imposed on the problem.

Using the kinematic and constitutive relations, the strain energy density function and consequently the total potential can be expressed solely in terms of the stress function, the normal component of the displacement, and their space-dependent derivatives.

Furthermore, solution of the compatibility equation, eqn (18), subject to boundary conditions, eqns (19) and (20) yields ψ in terms of w and its space dependent derivatives. Then, taking this expression for ψ, the total potential may be expressed solely in terms of normal component of displacement and its space dependent derivatives (all of the above mathematical steps are omitted for the sake of brevity).

$$\begin{aligned} U_T = \frac{\pi}{\beta_0}\int_0^R &\left\{\alpha_0^2\left(w_{,rr} + \frac{w_{,r}}{r}\right)^2 + \frac{\beta_0^2}{4}\left(\int_0^r \frac{w_{,x}^2}{x}dx\right)^2 + \left(\frac{2H\beta_0 w}{R^2}\right)^2 + C_0^2 + \left(w_{,rr} + \frac{w_{,r}}{r}\right)\left[2\alpha_0 C_0\right.\right. \\ &\left.\left. + \frac{4H}{R^2}\alpha_0\beta_0 w - \alpha_0\beta_0\int_0^r \frac{w_{,x}^2}{x}dx\right] - \left[\frac{2H}{R^2}\beta_0^2 w + C_0\beta_0\right]\int_0^r \frac{w_{,x}^2}{x}dx + \frac{4H}{R^2}\beta_0 C_0 w\right\} r\,dr \\ &- \frac{\pi}{\beta_0}\left(\frac{1+\lambda_0+\nu}{1+\lambda_0}\right)\left\{-\frac{\beta_0}{2R}\int_0^R r\left(\int_0^r \frac{w_{,x}^2}{x}dx\right)dr + \frac{2H\beta_0}{R^3}\int_0^R wr\,dr + \frac{C_0 R}{2}\right\}^2 \\ &- \pi\left\{\frac{(eE^s)^2}{\beta_0} - D\left(1 + \rho_0 + 12\lambda_0\frac{e^2}{h^2}\right)\right\}\int_0^R \left(w_{,r} + \frac{w_{,r}}{r}\right)^2 r\,dr - 2\pi\int_0^R qwr\,dr \end{aligned} \tag{21}$$

where

$$\alpha_0 = e\left(\frac{\lambda_0}{1+\lambda_0}\right)\nu E^p \tag{22}$$

$$\beta_0 = \frac{E^p}{1+\lambda_0}[(1+\lambda_0)^2 - \nu^2] \tag{23}$$

and

$$C_0 = \beta_0\left(\frac{1+\lambda_0+\nu}{1+\lambda_0-\nu}\right)\left\{\frac{1+\lambda_0}{1+\lambda_0+\nu}\int_0^R \frac{w_{,r}^2}{r}\,\mathrm{d}r - \frac{1}{R^2}\int_0^R r\left(\int_0^r \frac{w_{,x}^2}{x}\,\mathrm{d}x\right)\mathrm{d}r + \frac{4H}{R^4}\int_0^R rw\,\mathrm{d}r\right\}. \tag{24}$$

Nondimensionalization

It is convenient to nondimensionalize all dimensional quantities. The total potential is nondimensionalized by using the following relations

$$\xi = \frac{r}{R};\quad \eta = \frac{w}{h};\quad e_0 = \frac{H}{h};\quad \eta_0 = \frac{z}{h}\quad (\;)' = \frac{\mathrm{d}}{\mathrm{d}\xi};\quad \nabla_*^2 = \frac{\mathrm{d}^2}{\mathrm{d}\xi^2} + \frac{1}{\xi}\frac{\mathrm{d}}{\mathrm{d}\xi}; \tag{25}$$

$$Q(\xi,\tau) = \frac{(1-\nu^2)R^4}{Eh^4}q(r,t);$$

Using the quantities defined above, the following nondimensional expression for the total potential is obtained.

$$U_T^* = \frac{(1-\nu^2)R^2}{2\pi Eh^5}U_T. \tag{26}$$

Using the following non-dimensional constants

$$B_1 = \frac{e\lambda_0\nu}{h(1+\lambda_0)};\qquad B_2 = \frac{(1+\lambda_0)^2-\nu^2}{1+\lambda_0};\qquad B_3 = \frac{1+\lambda_0+\nu}{1+\lambda_0-\nu} \tag{27}$$

and the expression

$$B_0 = \frac{1+\lambda_0}{1+\lambda_0+\nu}\int_0^1 \frac{\eta_{,\xi}^2}{\xi}\,\mathrm{d}\xi - \int_0^1 \xi\left(\int_0^\xi \frac{\eta_{,x}^2}{x}\,\mathrm{d}x\right)\mathrm{d}\xi + 4e_0\int_0^1 \xi\eta\,\mathrm{d}\xi \tag{28}$$

the non-dimensional total potential can be written as

$$\begin{aligned}
U_T^* = {} & \frac{1}{2}\frac{B_1^2}{B_2}\int_0^1 (\nabla_*^2\eta)^2\xi\,\mathrm{d}\xi + \frac{B_2}{8}\int_0^1\left(\int_0^\xi \frac{\eta_{,x}^2}{x}\,\mathrm{d}x\right)^2\xi\,\mathrm{d}\xi + 2e_0^2B_2\int_0^1 \eta^2\xi\,\mathrm{d}\xi \\
& + \frac{1}{4}B_2B_3^2B_0^2 + B_1B_3B_0\int_0^1 \nabla_*^2\eta\xi\,\mathrm{d}\xi + 2e_0B_1\int_0^1 \eta\nabla_*^2\eta\xi\,\mathrm{d}\xi \\
& - \frac{B_1}{2}\int_0^1 \nabla_*^2\eta\left(\int_0^\xi \frac{\eta_{,x}^2}{x}\,\mathrm{d}x\right)\xi\,\mathrm{d}\xi - e_0B_2\int_0^1 \eta\left(\int_0^\xi \frac{\eta_{,x}^2}{x}\,\mathrm{d}x\right)\xi\,\mathrm{d}\xi \\
& - \frac{1}{2}B_2B_3B_0\int_0^1\left(\int_0^\xi \frac{\eta_{,x}^2}{x}\,\mathrm{d}x\right)\xi\,\mathrm{d}\xi + 2e_0B_2B_3B_0\int_0^1 \eta\xi\,\mathrm{d}\xi \\
& - \frac{1}{2}(1+\lambda_0+\nu)[(1+\lambda_0)^2-\nu^2]\left[\frac{B_0}{1+\lambda_0-\nu} - \frac{1}{2(1+\lambda_0+\nu)}\int_0^1 \frac{\eta_{,\xi}^2}{\xi}\,\mathrm{d}\xi\right]^2 \\
& - \frac{1}{24}\left\{12\frac{B_1^2}{B_2}\left(\frac{1+\lambda_0}{\nu}\right)^2 - \left(1+\rho_0+12\lambda_0\frac{e^2}{h^2}\right)\right\}\int_0^1 (\nabla_*^2\eta)^2\xi\,\mathrm{d}\xi - Q\int_0^1 \eta\xi\,\mathrm{d}\xi.
\end{aligned} \tag{29}$$

Nondimensionalized expression for U_T

The initial shape of the midsurface is assumed to be spherical and the meridional curve is approximated by the parabola

$$\eta_0(\xi) = e_0(1-\xi^2). \tag{30}$$

The spherical cap is assumed to be clamped along its circular boundary. Thus the boundary conditions on the normal displacement, w, in nondimensionalized form are

$$\eta(1,\tau)=0;\quad \eta'(1,\tau)=0;\quad \text{where}\quad (\ )'=\frac{d}{d\xi}. \tag{31}$$

The nondimensional vertical displacement, η, is expressed in terms of the following series

$$\eta=\sum_{n=1}^{\infty} a_n(\tau)[J_0(k_n{}^1\xi)-J_0(k_n{}^1)] \tag{32}$$

where $k_n{}^1$ are the zeroes of $J_1(x)=0$ and each term of the series satisfies the boundary conditions, eqns (31). The functions $[J_0(k_n{}^1\xi)-J_0(k_n{}^1)]$ represent the axisymmetric buckling modes of an eccentrically stiffened flat circular plate loaded by a uniformly applied edge thrust[34]. For the dynamic case considered, the time-dependent coefficients, $a_n(\tau)$, are thought of as generalized coordinates and the time history of the displacement is defined in terms of these coordinates. For the quasi-static case, however, these coefficients become undetermined constants.

It is convenient now to define and/or evaluate certain integrals which occur in the expression for the total potential energy, eqn (29). Using well-known properties of Bessel functions, the following relations for the integrals are obtained (the superscript "1" on k_n is dropped for convenience)

$$\int_0^1 (\nabla_*^2\eta)^2\xi\,d\xi=\frac{1}{2}\sum_{n=1}^{\infty} a_n{}^2k_n{}^4J_0{}^2(k_n) \tag{33}$$

and

$$\int_0^\xi \frac{\eta_{,x}^2}{x}\,dx=\sum_{n=1}^{\infty}\sum_{m=1}^{\infty} a_na_m\varphi_{nm}(\xi) \tag{34}$$

where

$$\varphi_{nm}(\xi)=\int_0^\xi \frac{k_nk_m}{x}J_1(k_mx)J_1(k_nx)\,dx \tag{35}$$

also by defining

$$\gamma_{nmpq}=\int_0^1 \varphi_{nm}(\xi)\varphi_{pq}(\xi)\xi\,d\xi. \tag{36}$$

The following expression is obtained

$$\int_0^1 \xi\left(\int_0^\xi \frac{\eta_{,x}^2}{x}\,dx\right)^2 d\xi=\sum_{n=1}^{\infty}\sum_{m=1}^{\infty}\sum_{p=1}^{\infty}\sum_{q=1}^{\infty} a_na_ma_pa_q\gamma_{nmpq} \tag{40}$$

and it can be shown that

$$\int_0^1 \eta^2\xi\,d\xi=\frac{1}{2}\sum_{n=1}^{\infty} a_n{}^2J_0{}^2(k_n)+\frac{1}{2}\sum_{n=1}^{\infty}\sum_{m=1}^{\infty} a_na_mJ_0(k_n)J_0(k_m) \tag{41}$$

$$\int_0^1 \nabla_*^2\eta\xi\,d\xi=0 \tag{42}$$

$$\int_0^1 \eta\nabla_*^2\eta\xi\,d\xi=-\frac{1}{2}\sum_{n=1}^{\infty} a_n{}^2k_n{}^2J_0{}^2(k_n) \tag{43}$$

$$\int_0^1 \eta\xi\,d\xi=-\frac{1}{2}\sum_{n=1}^{\infty} a_nJ_0(k_n) \tag{44}$$

$$\int_0^1 \xi\left(\int_0^\xi \frac{\eta_{,x}^2}{x}\,dx\right)d\xi=\sum_{n=1}^{\infty}\sum_{m=1}^{\infty} a_na_m\alpha_{nm} \tag{45}$$

$$\int_0^1 \eta\left(\int_0^\xi \frac{\eta_{,x}^2}{x}\mathrm{d}x\right)\xi\mathrm{d}\xi = \sum_{n=1}^{\infty}\sum_{m=1}^{\infty}\sum_{p=1}^{\infty} a_n a_m a_p[\tau_{nmp} - J_0(k_n)\alpha_{mp}] \tag{46}$$

$$\int_0^1 \nabla_*^2\eta\left(\int_0^\xi \frac{\eta_{,x}^2}{x}\mathrm{d}x\right)\xi\mathrm{d}\xi = -\sum_{n=1}^{\infty}\sum_{m=1}^{\infty}\sum_{p=1}^{\infty} a_n a_m a_p k_n^2\tau_{nmp} \tag{47}$$

where

$$\alpha_{nm} = \int_0^1 \xi\varphi_{nm}(\xi)\mathrm{d}\xi \tag{48}$$

$$\tau_{nmp} = \int_0^1 J_0(k_n\xi)\varphi_{mp}(\xi)\xi\mathrm{d}\xi. \tag{49}$$

By using the integrals defined above, the total potential may be expressed as a polynomial of fourth order in the generalized coordinates.

$$\begin{aligned}
U_T^* = {} & \frac{1}{4}\frac{B_1^2}{B_2}\sum_{n=1}^{\infty} a_n^2k_n^4J_0^2(k_n) + \frac{B_2}{8}\sum_{n=1}^{\infty}\sum_{m=1}^{\infty}\sum_{p=1}^{\infty}\sum_{q=1}^{\infty} a_na_ma_pa_q\gamma_{nmpq} \\
& + e_0^2B_2\left[\sum_{n=1}^{\infty} a_n^2J_0^2(k_n) + \sum_{n=1}^{\infty}\sum_{m=1}^{\infty} a_na_mJ_0(k_n)J_0(k_m)\right] + \frac{1}{4}B_2B_3^2B_0^2 \\
& - e_0B_1\sum_{n=1}^{\infty} a_n^2k_n^2J_0^2(k_n) + \frac{B_1}{2}\sum_{n=1}^{\infty}\sum_{m=1}^{\infty}\sum_{p=1}^{\infty} a_na_ma_pk_n^2\tau_{nmp} \\
& - e_0B_2\sum_{n=1}^{\infty}\sum_{m=1}^{\infty}\sum_{p=1}^{\infty} a_na_ma_p[\tau_{nmp} - J_0(k_n)\alpha_{mp}] \\
& - \frac{1}{2}B_2B_3B_0\sum_{n=1}^{\infty}\sum_{m=1}^{\infty} a_na_m\alpha_{nm} - e_0B_2B_3B_0\sum_{n=1}^{\infty} a_nJ_0(k_n) \\
& - \frac{(1+\lambda_0+\nu)}{2}[(1+\lambda_0)^2-\nu^2]\left[\frac{B_0}{1+\lambda_0-\nu} - \frac{1}{2(1+\lambda_0+\nu)}\sum_{n=1}^{\infty}\sum_{m=1}^{\infty} a_na_m\varphi_{nm}(1)\right]^2 \\
& - \frac{1}{48}\left\{12\frac{B_1^2}{B_2}\left(\frac{1+\lambda_0}{\nu}\right)^2 - \left(1+\rho_0+12\lambda_0\frac{e^2}{h^2}\right)\right\}\sum_{n=1}^{\infty} a_n^2k_n^4J_0^2(k_n) + \frac{Q}{2}\sum_{n=1}^{\infty} a_nJ_0(k_n)
\end{aligned} \tag{50}$$

where

$$B_0 = \frac{1+\lambda_0}{1+\lambda_0+\nu}\sum_{n=1}^{\infty}\sum_{m=1}^{\infty} a_na_m\varphi_{nm}(1) - \sum_{n=1}^{\infty}\sum_{m=1}^{\infty} a_na_m\alpha_{nm} - 2e_0\sum_{n=1}^{\infty} a_nJ_0(k_n). \tag{51}$$

4. LINEAR ANALYSIS FOR THE COMPLETE SPHERE

A linear analysis was performed on a complete sphere geometry similar to that used for the spherical cap under quasi-statically applied uniform pressure. The buckling equation is derived by allowing a primary state to exist and through linearization of the equilibrium equations by assuming that the additional buckled state parameters are small by comparison to the primary state parameters (bifurcation approach). Thus the problem is reduced to an eigenvalue problem. The solution to the buckling equations can be written in terms of spherical harmonics and the characteristic equation is (for more details see[2]).

$$\begin{aligned}
\frac{qa(1-\nu^2)}{2Eh}\Big[& -n^2(n+1)^2\left(1+\lambda_0+\lambda_0\frac{e}{a}\right) + n(n+1)\left(1-\nu+\lambda_0+4\lambda_0\frac{e}{a}\right) \\
& + 2(1+\nu+\lambda_0)\Big] - n^3(n+1)^3\left[\left\{1+\alpha\rho_0+\lambda_0\left(1+\frac{e}{a}\right)^2\right\}\left\{\alpha(1+\rho_0)\right.\right. \\
& \left.\left. + \lambda_0\frac{e^2}{a^2}\right\} - \left\{\alpha(1+\rho_0)+\lambda_0\frac{e}{a}\left(1+\frac{e}{a}\right)^2\right\}\right] \\
& + n^2(n+1)^2\left[\left\{1+\alpha\rho_0+\lambda_0\left(1+\frac{e}{a}\right)^2\right\}\left\{\alpha(1+\rho_0-\nu)-\lambda_0\frac{e}{a}\left(2-\frac{e}{a}\right)\right\}\right.
\end{aligned}$$

$$
\begin{aligned}
&+\left\{1-\nu+\alpha\rho_0+\lambda_0\left(1+\frac{e}{a}\right)^2\right\}\left\{\alpha(1+\rho_0)+\lambda_0\frac{e^2}{a^2}\right\} \\
&+2\left\{\alpha(1+\rho_0)+\lambda_0\frac{e}{a}\left(1+\frac{e}{a}\right)\right\}\left\{1+\nu-\alpha\rho_0+\lambda_0\left(1-\frac{e^2}{a^2}\right)\right\}\Bigg] \\
&-n(n+1)\Bigg[2(1+\nu+\lambda_0)\left\{1+\alpha\rho_0+\lambda_0\left(1+\frac{e}{a}\right)^2\right\} \\
&+\left\{\alpha(1-\nu+\rho_0)-\lambda_0\frac{e}{a}\left(2-\frac{e}{a}\right)\right\}\left\{1-\nu+\alpha\rho_0+\lambda_0\left(1+\frac{e}{a}\right)^2\right\} \\
&-\left\{1+\nu-\alpha\rho_0+\lambda_0\left(1-\frac{e^2}{a^2}\right)\right\}^2\Bigg]+2(1+\nu+\lambda_0)\left[1-\nu+\alpha\rho_0+\lambda_0\left(1+\frac{e}{a}\right)^2\right]=0
\end{aligned}
\tag{52}
$$

where $\alpha = h^2/12a^2$, and n is the degree of the spherical harmonics. The above characteristic equation corresponds to the case for which the load remains normal to the deflected midsurface during buckling.

Critical loads are obtained through minimization of q with respect to integer values of n.

5. NUMERICAL SOLUTION AND RESULTS

Linear analysis

A computer program was written and numerical results were obtained for three geometric configuration denoted by (a) light stiffening, (b) moderate stiffening, and (c) strong stiffening. The Georgia Tech Univac 1108 high speed digital computer was used for this purpose. These results are presented in graphical form in Fig. 3. The percent weight savings is obtained by comparing the weight of an isotropic spherical shell, which has the same critical pressure as the stiffened shell, to the weight of the stiffened shell. In Fig. 3 the load has been divided by the classical critical pressure for a sphere of thickness h.

Spherical cap

Two-term solutions are obtained and the results are presented as plots of the ratio of critical

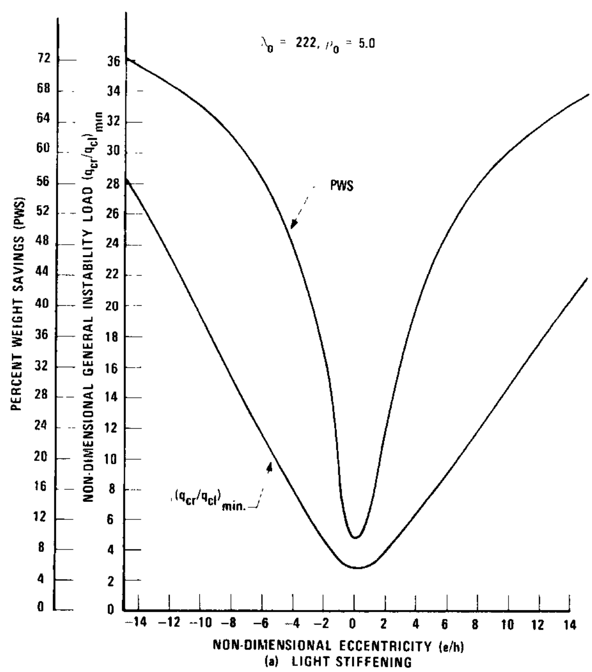

Fig. 3a. General instability results of linear analysis. (Light stiffening).

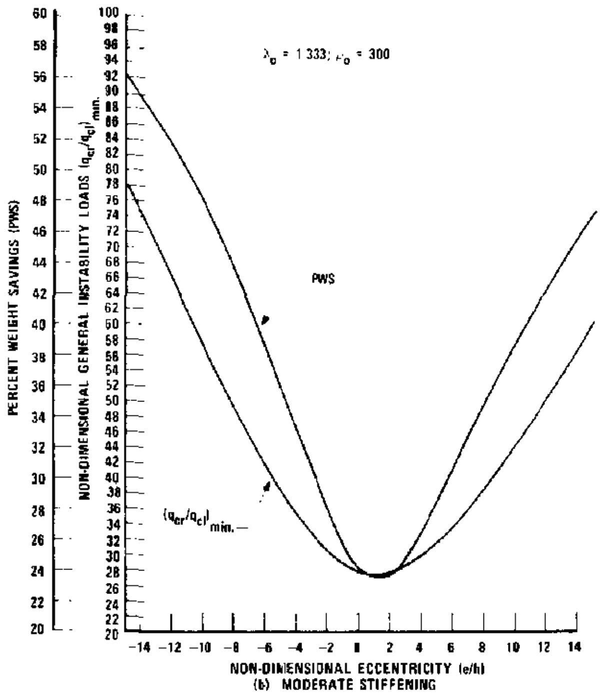

Fig. 3b. General instability results of linear analysis. (Moderate stiffening).

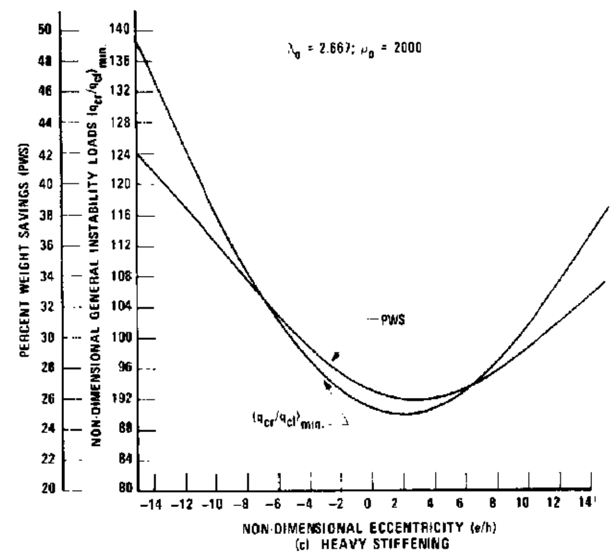

Fig. 3c. General instability results of linear analysis. (Heavy stiffening).

pressure to complete spherical shell critical pressure versus the initial rise parameter given by

$$\lambda = 2[3(1-\nu^2)]^{1/4}\left(\frac{H}{h_{eq}}\right)^{1/2}$$

where h_{eq} is the sum of the sheet and stiffener smeared thicknesses.

The two-term approximation appears to be a good approximation for the range of λ-values for which axisymmetric response prevails.

In Fig. 4 results for the quasi-static case are presented for the same geometric configurations as in the linear analysis. In addition, the isotropic geometry is used to establish the validity of the two-term solution.

In Fig. 5 results for the dynamic case are presented for the same geometric configurations.

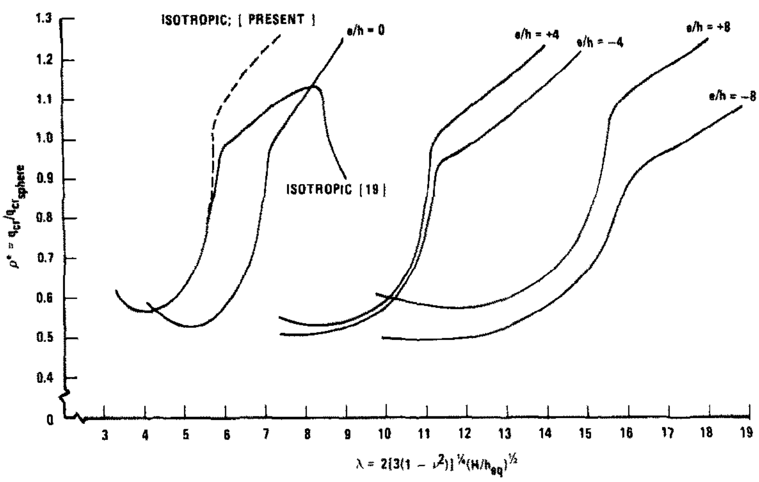

Fig. 4a. Critical pressure ratio, ρ, vs initial rise parameter, λ, (quasi-static). (Isotropic and light stiffening).

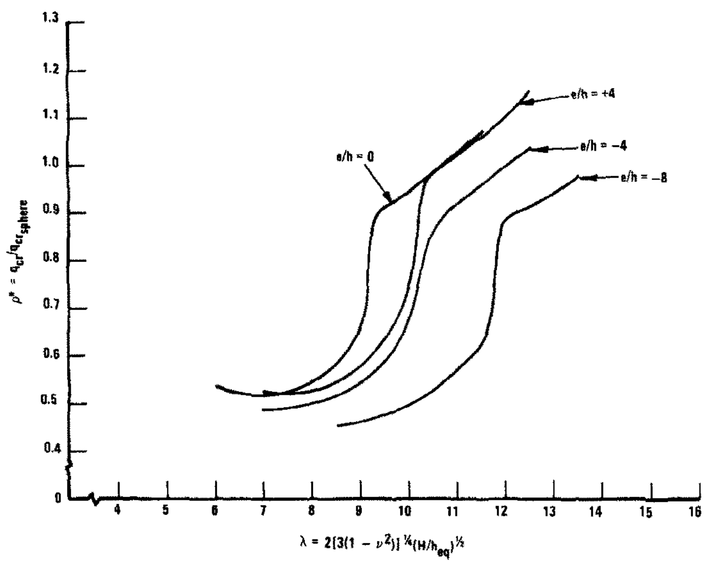

Fig. 4b. Critical pressure ratio, ρ, vs initial rise parameter, λ, (quasi-static). Moderate stiffening.

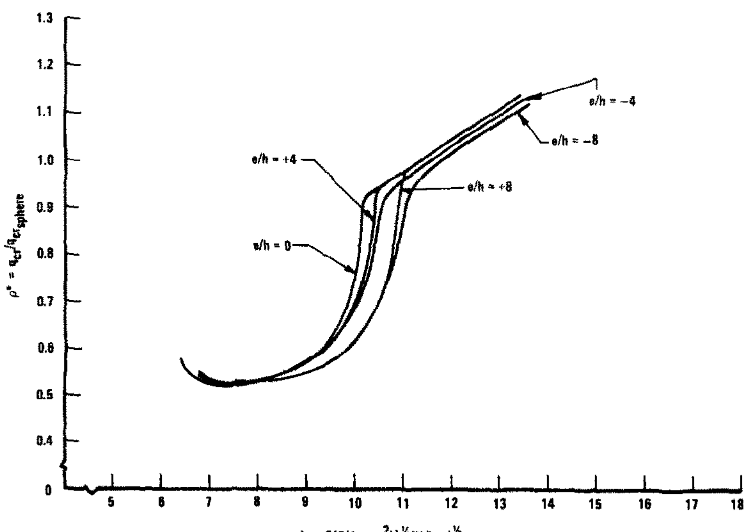

Fig. 4c. Critical pressure ratio, ρ, vs initial rise parameter, λ, (quasi-static). (Heavy stiffening).

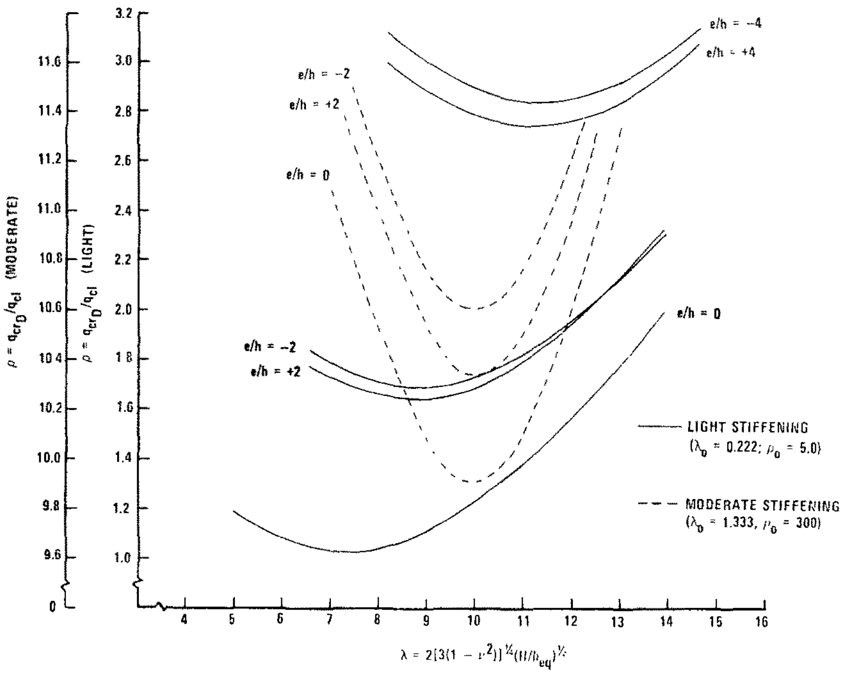

Fig. 5a. Critical pressure ratio, ρ, vs initial rise parameter, λ (dynamic constant load, infinite duration). Light and moderate stiffening.

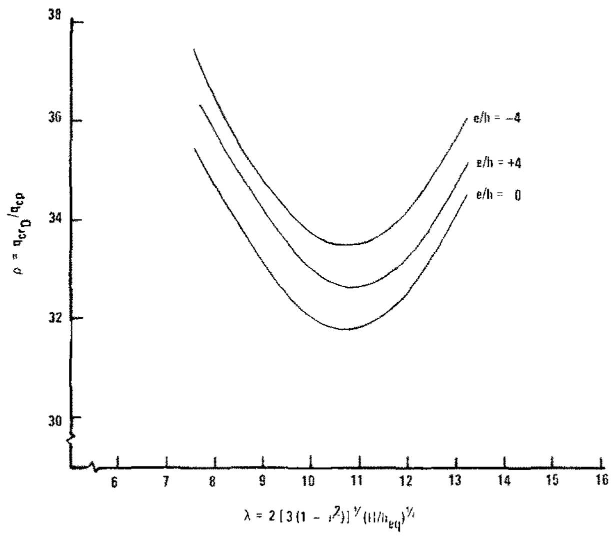

Fig. 5b. Critical pressure ratio, ρ, vs initial rise parameter, λ (dynamic constant load, infinite duration). Heavy stiffening.

6. CONCLUSIONS

By studying the generated data the following important conclusions may be drawn:

(1) For quasi-statically applied pressure on the complete sphere, inside stiffeners yield a stronger configuration than outside stiffeners (see Fig. 3). This is also true for the spherical cap for the range of λ-values considered, but the effect diminishes as the eccentricity increases. Note from Fig. 4 that the positive eccentricity curve lies above the negative eccentricity curve which might suggest the reverse effect, but it is not so because of the normalizing factor (q_{cr} for the complete sphere).

(2) In order to sustain a given uniformly distributed pressure, the isotropic complete spherical shell must be heavier than the stiffened shell. This savings increases with eccentricity. This effect is verified for a number of spherical cap geometries (spot-checked).

(3) For the dynamic load case, snap-through is possible for λ-values higher than some

minimum λ. This minimum λ-value is approximately 3·2 for the isotropic geometry and it increases with eccentricity for each configuration.

(4) For the dynamic case, inside stiffening yields a stronger configuration than outside stiffening for the lower values of λ. A reversal of this phenomenon might take place at some value of λ as suggested by the curves (see Fig. 5).

(5) The critical dynamic load is smaller than the quasi-statically applied critical load. The reduction is anywhere from 20% to 65% depending on the initial rise parameter for the isotropic geometry [9]. The same is true for the stiffened geometries with a slight dependence on stiffener positioning. The upper limit of reduction is greater for inside stiffener configurations.

REFERENCES

1. O. Harari, J. Singer and J. Baruch, General Instability of Cylindrical Shells with Non-uniform Stiffeners. *Israel J. Tech.* **5**, 114 (1967).
2. R. T. Cole, *An Analysis on the General Instability of Eccentrically Stiffened Complete Spheres under Pressure.* Ph.D. Thesis, Georgia Institute of Technology, Atlanta, Georgia (1969).
3. A. Van der Neut, The General Instability of Stiffened Cylindrical Shells under Azial Compression. National Luchtvaartlaboratorium Rept. S314, Vol. XIII, pp. 557–584. Amsterdam, the Netherlands (1947).
4. Th. Von Kármán and H. S. Tsien, The buckling of spherical shells by external pressure. *J. Aeronautical Sciences.* **7**, 43 (1939).
5. J. Suhara, *Snapping of Shallow Spherical Shells Under Static and Dynamic Loadings.* Aeroelastic and Structures Research Laboratory, ASRL TR 76-4, MIT (June 1960).
6. J. S. Humphreys and S. R. Bodner, Dynamic buckling of shallow shells under impulsive loading. *J. Engng Mech. Division, Proc. Amer. Soc. Civil Engers.* **88**, EM 2, 17 (April 1962).
7. B. Budiansky and R. S. Roth, *Axisymmetric Dynamic Buckling of Clamped Shallow Spherical Shells.* pp. 597–606. NASA TN D-1510 (1962).
8. R. R. Archer and C. G. Lange, Nonlinear dynamic behavior of shallow spherical shells. *AIAA Journal*, **3**, 2313 (1965).
9. G. J. Simitses, Axisymmetric dynamic snap-through buckling of shallow spherical caps. *AIAA Journal*, **5**, 1019 (1967); (see also Proc. *ASME/AIAA 7th Structures and Materials Conf.*, Cocoa Beach, Florida, 1966).
10. J. H. Lock, S. Okubo and J. S. Whittier, Experiments on the snapping of a shallow dome under a step pressure load. *AIAA Journal*, **6**, 1320 (1968).
11. W. B. Stephens and R. E. Fulton, *Axisymmetric Static and Dynamic Buckling of Spherical Caps due to Centrally Distributed Pressures.* AIAA Paper, 69–89 (1969).
12. J. A. Stricklin and J. E. Martinez, Dynamic buckling of clamped spherical caps under step pressure loadings. *AIAA J.* **7**, 1212 (1969).
13. J. C. Huang, Axisymmetric dynamic snap-through of elastic clamped shallow spherical shells. *AIAA Journal*, **7**, 215 (1969).
14. G. J. Simitses, On the dynamic buckling of shallow spherical shells. *J. Appl. Mech.* **41**, 299 (1974).
15. A. A. Liepins, *Asymmetric Nonlinear Dynamic Response and Buckling of Shallow Spherical Shells.* NASA CR-1376, (June 1969).
16. T. L. Lin, C. D. Babcock, *An Energy Approach to the Dynamic Buckling of Spherical Caps.* AFORSR TR-71-1076 (or GALCIT SM71-72) (April 1971).
17. J. Mescall and T. Tsui, Influence of damping on the dynamic stability of spherical caps under step pressure loading. *AIAA Journal*, **9**, 1244 (1971).
18. J. M. Klosner and R. Longhitamo, Nonlinear Dynamics of Hemispherical Shells. *AIAA Journal*, **11**, 1117 (1973).
19. P. G. Glockner and K. Z. Tawadros, Experiments on free vibrations of shells of revolution. *Experimental Mechanics*, **13**, 411 (1973).
20. M. Sunakawa and K. Ichida, *A High Precision Experiment on the Buckling of Spherical Caps Subjected to External Pressure.* Institute of Space and Aeronautical Sciences, University of Tokyo, ISAS Report No. 508 (Vol. 39, No. 5), (March 1974).
21. A. Kaplan, Buckling of spherical shells, *Thin-Shell Structures, Theory, Experiment and Design*, (Edited by Y. C. Fung and E. E. Sechler), pp. 247–288. Prentice-Hall, Englewood Cliffs, N. J. (1974).
22. D. Bushnell, Nonlinear Axisymmetric Behavior of shells of revolution. *AIAA Journal*, **5**, 432 (1967).
23. D. Bushnell, Symmetric and nonsymmetric buckling of finitely deformed eccentrically stiffened shells of revolution. *AIAA Journal*, **5**, 1455 (1967).
24. H. Ebner, Angenaherte bestimmung der tragfahigkeit radial versteifter kugelschalen unter druckbelnstugn. *Proceedings of the Symposium on the Theory of Thin Elastic Shells*, (Edited by W. T. Koiter), pp. 95–121. North-Holland, Amsterdam (1960).
25. R. F. Crawford and D. B. Schwartz, General instability and optimum design of grid-stiffened spherical domes. *AIAA Journal*, **3**, 511 (1965).
26. R. F. Crawford, *Effects of Asymmetric Stiffening on Buckling of Shells.* AIAA Paper 65–371 (1965).
27. B. Budiansky, Buckling of clamped shallow spherical shells. *Proceeding of the Symposium on the Theory of Thin Elastic Shells*, (Edited by W. T. Koiter), pp. 64–94. North-Holland, Amsterdam (1960).
28. E. Reissner, On axisymmetric vibrations of shallow spherical shells. *Qua. Appl. Math.* **13**, 279 (1955).
29. E. Reissner, On transverse Vibrations of thin shallow elastic shells. *Qua. Appl. Math.* **13**, 169 (1955).
30. J. S. Humphreys, On the adequacy of energy criteria for dynamic buckling of arches. *AIAA Journal*, **4**, 921 (1966).
31. J. L. Sanders Jr., Nonlinear Theories for Thin Shells, *Qua. Appl. Math.* **21**, 21 (1963).
32. M. Baruch and J. Singer, Effect of Eccentricity of Stiffeners on the General Instability of Stiffened Cylindrical shells under Hydrostatic Pressure. *Mech. Eng. Sic.* **5**, 23 (1963).
33. N. C. Huang, Unsymmetrical Buckling of Thin Shallow Spherical Shells, *J. Appl. Mech.* 447 (1964).
34. G. J. Simitses and C. M. Blackmon, Buckling of eccentrically stiffened thin circular plates. *AIAA Journal*, **7**, 1200 (1969).